The current issue and full text archive of this journal is available at
http://www.emeraldinsight.com/0961-5539.htm

A moving grid model for the pyrolysis of charring materials

E. Theuns, J. Vierendeels and P. Vandevelde
Department of Flow, Heat and Combustion Mechanics, Ghent University, Belgium

Received September 2001
Accepted February 2002

Keywords *Pyrolysis, Moving boundary, Model*

Abstract *This paper describes a one dimensional moving grid model for the pyrolysis of charring materials. In the model, the solid is divided by a pyrolysis front into a char and a virgin layer. Only when the virgin material reaches a critical temperature it starts to pyrolyse. The progress of the front determines the release of combustible volatiles by the surface. The volatiles, which are produced at the pyrolysis front, flow immediately out of the solid. Heat exchange between those volatiles and the char layer is taken into account. Since the model is used here as a stand-alone model, the external heat flux that heats up the solid, is assumed to be known. In the future, this model will be coupled with a CFD code in order to simulate fire spread. The char and virgin grid move along with the pyrolysis front. Calculations are done on uniform and on non-uniform grids for the virgin layer. In the char layer only a uniform grid is used. Calculations done with a non-uniform grid are about 3 times faster than with a uniform gird. The moving grid model is compared with a faster but approximate integral model for several cases. For sudden changes in the boundary conditions, the approximate integral model gives significant errors.*

Notation

a = mesh growth factor [−]
c = specific heat capacity [J/kg.K]
E = internal energy [J/kg]
ΔH_{pyr} = latent heat of vaporisation/pyrolysis [J/kg]
i = node number
L = total thickness of solid [m]
$\dot{m}''$ = mass flux [kg/m^2.s]
$\vec{n}$ = normal at surface S
N = number of cells
p = pressure [Pa]
$\dot{q}''$ = heat flux [W/m^2]
$\dot{q}''_c$ = heat flux from the char layer to pyrolysis front [W/m^2]
$\dot{q}''_{flame}$ = heat flux from the flame to the solid [W/m^2]
$\dot{q}''_{net}$ = net incident heat flux at surface of solid [W/m^2]
$\dot{q}''_v$ = heat flux from pyrolysis front to virgin material [W/m^2]
$\dot{q}'''$ = generated heat density [W/m^3]
T = temperature [K]
t = time [s]
v = velocity [m/s]
w = mesh velocity [m/s]
x = distance from front surface [m]

Greek symbols
α = thermal diffusivity [m^2/s]
δ = thickness of char or virgin layer [m]
ε = emissivity of solid surface
θ = parameter controlling type of difference scheme
λ = thermal conductivity [W/m.K]
ρ = density [kg/m^3]
σ = Stefan-Boltzmann constant [W/m^2.K^4]

Subscripts
bs = back surface
c = char
ext = external

International Journal of Numerical Methods for Heat & Fluid Flow, Vol. 12 No. 5, 2002, pp. 541-559.

DOI 10.1108/09615530210434287

E = east or right node
fr = pyrolysis front
g = pyrolysis gasses
pyr = pyrolysis
s = surface
v = virgin
W = west or left node
∞ = environment

Introduction

Fire can be seen as an unwanted combustion. It affects society and environment by loss of life and property. Simulations can give insight in the mechanism of initiation and growth of a fire. A drawback of most of today's compartment fire models, typical zone and CFD models, is that the fire has to be predefined. The progress of the fire with time is defined before the calculation, and is independent of the conditions in the enclosure during the simulation. Models that can predict the fire growth itself, from only an initiating fire (e.g. burning cigarette), would expand substantially the utility of fire models.

Flame spread can be seen as an advancing ignition front. Flames or other heat sources, heat up the virgin combustible material. With increasing temperature, the material starts to pyrolyse and a char layer is formed. The pyrolysis gasses or combustible volatiles flow to the surface of the solid and burn or ignite in the gas phase. The reaction of the solid material to the incident heat flux is important for the modelling of the fire spread or growth.

There exist different models that describe the pyrolysis of charring materials, going from simple analytical equations (Tewarson, 1995) to complex coupled partial differential equations where the thermal degradation reactions are often modelled with a first order Arrhenius equation (Di Blasi, 1994) (Staggs, 2000). In the model that will be described here, the pyrolysis zone is modelled as a infinitely thin surface. Hence a coarser grid can be used than in (Di Blasi, 1994), where the pyrolysis front has a finite thickness and finer grids are required.

The moving grid technique is used because it is conservative, unlike the front-fixing finite difference method using for example a Landau transformation. The model will be incorporated into a CFD code and used as a boundary condition.

In a real fire, or in a fire test, the solid is heated mainly by radiation and convection. The incident heat flux comes from an external heater, e.g. radiating cone in the Cone Calorimeter test, flames at the solid surface, a hot gas layer, etc. In this paper, the model is used as a stand-alone model. Therefore, the net incident heat flux has to be supplied as a boundary condition. When the solid model will be coupled to a CFD code, this net incident heat flux will be computed by the code.

Model description

The pyrolysis front is modelled as a surface with zero thickness. During pyrolysis the char and virgin zones are always separated from each other by this pyrolysis front. Each zone consists of only one material (virgin or char) and has constant thermal parameters. The temperature at the pyrolysis front is constant and is assumed a material property. The volatiles produced at the pyrolysis front, flow immediately out of the solid (Spearpoint and Quintiere, 2000) (Yan and Holmstedt, 1997). Calculations are done with a one dimensional model.

Conservation equations

The conservation equation for mass expressed on a moving volume V, with surface S, is given by:

$$\frac{\mathrm{d}}{\mathrm{d}t}\int_V \rho \mathrm{d}V + \int_S \rho(\vec{v} - \vec{w})\cdot\vec{n}\mathrm{d}S = 0 \tag{1}$$

Similarly, the conservation equation for energy expressed on a moving volume V is given by:

$$\frac{\mathrm{d}}{\mathrm{d}t}\int_V \rho E \mathrm{d}V + \int_S \rho E(\vec{v} - \vec{w})\cdot\vec{n}\mathrm{d}S = \int_V \dot{q}'''\mathrm{d}V - \int_S \vec{\dot{q}}''\cdot n \rightarrow \mathrm{d}S \tag{2}$$

As there are no volatiles stored in the solid ($\rho_g = 0$ and $v_g = \infty$ but $\rho_g.v_g = \dot{m}''_g$), and after neglecting of the kinetic and the potential energy, the conservation of energy for the char layer for one dimensional pyrolysis, gives:

$$\frac{\mathrm{d}}{\mathrm{d}t}\int_0^{\delta_c} (\rho_c.c_c.T).\mathrm{d}x + \dot{m}''_g.c_g.T_s - \dot{m}''_g.c_g.T_{pyr} + (\rho_c.c_c.T_{pyr}).\left(-\frac{\mathrm{d}\delta_c}{\mathrm{d}t}\right) = \dot{q}''_{net} - \dot{q}''_c \tag{3}$$

The boundary conditions for the char layer are:

$$\begin{cases} -\lambda_c.\left.\dfrac{\mathrm{d}T}{\mathrm{d}x}\right|_{x=0} = \dot{q}''_{net} = \dot{q}''_{ext} + \dot{q}''_{flame} - \varepsilon.\sigma.(T_s^4 - T_\infty^4) \\ T|_{x=\delta_c} = T_{pyr} \end{cases} \tag{4}$$

In a similar way, for the virgin material (between $x = \delta_c$ and $x = L$), the conservation equation of energy becomes:

$$\frac{\mathrm{d}}{\mathrm{d}t}\int_{\delta_c}^{L} \rho_v.c_v.T\mathrm{d}x + \rho_v.c_v.T_{pyr}.\frac{\mathrm{d}\delta_c}{\mathrm{d}t} = \dot{q}''_v \tag{5}$$

The back surface is insulated. The boundary conditions of the virgin layer are given by:

$$\begin{cases} T|_{x=\delta_c} = T_{pyr} \\ \lambda_v . \left.\dfrac{\partial T}{\partial x}\right|_{x=L} = 0 \end{cases} \tag{6}$$

The char layer and the virgin material are coupled with each other by the pyrolysis front (at $x = \delta_c$). Although the pyrolysis front is assumed infinitely thin ($V = 0$), the conservation equations are still applicable. The conservation of mass gives:

$$(\rho_v - \rho_c) \cdot \frac{d\delta_c}{dt} = \dot{m}''_g \tag{7}$$

At the pyrolysis front heat will be absorbed by the chemical degradation reactions. The conservation of energy gives:

$$(\rho_v - \rho_c) \cdot \frac{d\delta_c}{dt} \cdot \Delta H_{pyr}(T_{pyr}) = \dot{q}''_c - \dot{q}''_v \tag{8}$$

Similar equations have been derived by (Moghtaderi *et al.*, 1997) and (Spearpoint and Quintiere, 2000).

Phases in simulation

For the moving grid method, three different phases have to be defined:

(1) heating up of the virgin material;

(2) pyrolysis;

(3) heating up of the char layer.

In the first phase, the solid consists entirely of virgin material. It is heated until the surface temperature reaches the pyrolysis temperature. After the onset of pyrolysis, the solid consists of char and virgin material. The pyrolysis front advances through the solid. When all the virgin material is burned, and thus the pyrolysis front has reached the solids back surface, the third phase starts. The solid consists now entirely of char material. The different phases and critical temperatures are given in Figure 1. Remark that the temperature profiles in Figure 1 are illustrative and not based on results.

Discretized equations

Mesh

In the char layer a uniform mesh is used, while for the virgin layer both uniform (Figure 2) and non-uniform meshes (Figure 3) have been used.

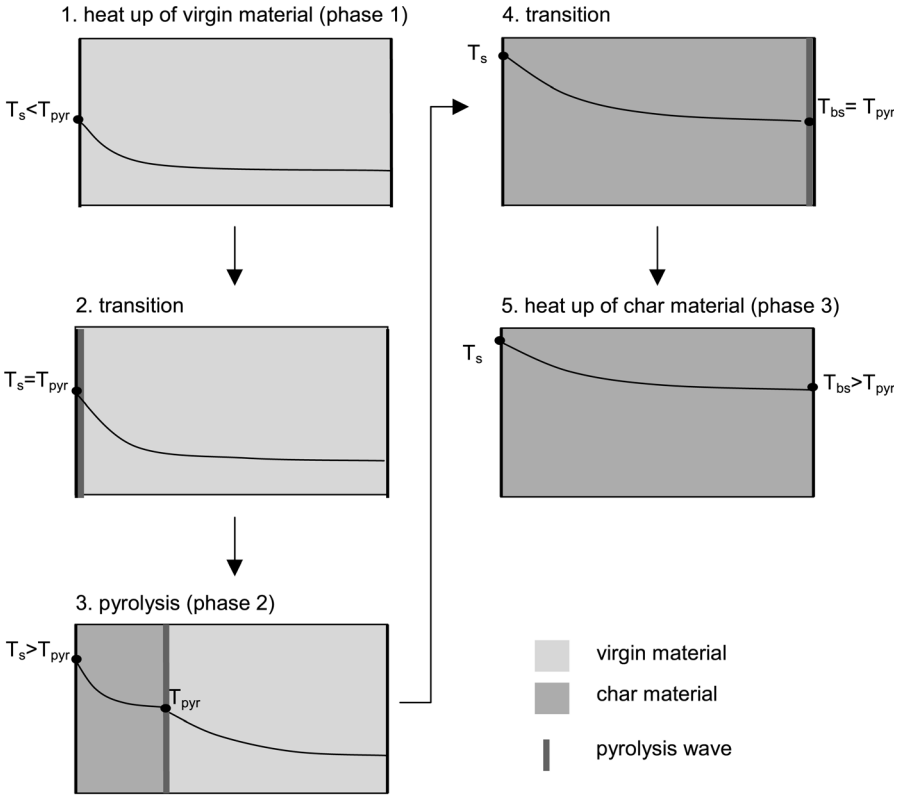

Figure 1.
Phases and temperature profiles during simulation

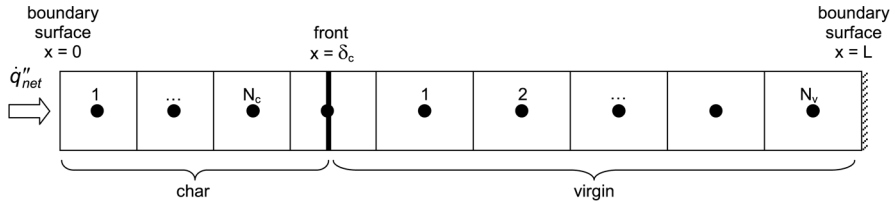

Figure 2.
Uniform mesh during pyrolysis

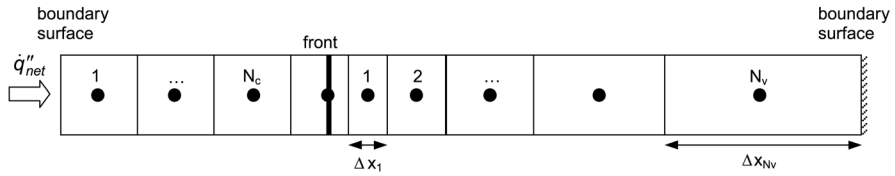

Figure 3.
Non uniform mesh during pyrolysis

During the pyrolysis phase the front temperature is known. It is the so-called pyrolysis temperature. As the virgin and the char layer both end at that front, a half-cell is taken so that a node can be placed at the front (Croft and Lilley, 1977). An example of the subsequent mesh is given for a uniform mesh in Figure 2, and for a non-uniform mesh in Figure 3. Notice that the cell size in the char zone is different than in the virgin zone.

As was done for the whole char layer, the conservation of energy, equation (2), can be applied for a single char cell:

$$\frac{\mathrm{d}}{\mathrm{d}t}\int_{\Delta x_i}(\rho_{\mathrm{c}}.c_{\mathrm{c}}.T).\mathrm{d}x + \dot{m}''_{\mathrm{g}}.c_{\mathrm{g}}.(T_{\mathrm{W}} - T_{\mathrm{E}}) - (\rho_{\mathrm{c}}.c_{\mathrm{c}}.).(w_{\mathrm{W}}.T_{\mathrm{W}} - w_{\mathrm{E}}.T_{\mathrm{E}}) = \dot{q}''_{\mathrm{E}} - \dot{q}''_{\mathrm{W}} \tag{9}$$

and for a virgin cell:

$$\frac{\mathrm{d}}{\mathrm{d}t}\int_{\Delta x_i}(\rho_{\mathrm{v}}.c_{\mathrm{v}}.T).\mathrm{d}x - (\rho_{\mathrm{v}}.c_{\mathrm{v}}.).(w_{\mathrm{W}}.T_{\mathrm{W}} - w_{\mathrm{E}}.T_{\mathrm{E}}) = \dot{q}''_{\mathrm{E}} - \dot{q}''_{\mathrm{W}} \tag{10}$$

where T_{W} and T_{E} are the temperatures, and w_{W} and w_{E} the boundary velocities at west and east boundary respectively.

Time discretization

Details about the discretization in time are only given for the pyrolysis phase. The discretized equations for the heating up phases can easily be deduced from the pyrolysis phase.

At the transition to the pyrolysis phase, the model equations are singular because the char zone does not yet exist. The problem of solving this singularity can simply be overcome by taking a first order fully implicit time step, only for the first time step in the pyrolysis phase. For the subsequent time steps, the second order accurate Cranck-Nicolson method is used. Heating of the pyrolysis gasses by the char layer can be included. To calculate a new time step at $n+1$, equation (9) is written out at a time level $n+\theta$:

$$\rho_{\mathrm{c}}c_{\mathrm{c}}\frac{T^{n+1}\Delta x^{n+1} - T^{n}\Delta x^{n}}{\Delta t} + \rho_{\mathrm{c}}c_{\mathrm{c}}(T_{\mathrm{W}}^{n+\theta}w_{\mathrm{W}}^{n+1/2} - T_{\mathrm{E}}^{n-\theta}w_{\mathrm{E}}^{n-1/2}) + \dot{m}''^{\,n+1/2}_{\mathrm{g}}c_{\mathrm{g}}(T_{\mathrm{W}}^{n+\theta} - T_{\mathrm{E}}^{n+\theta}) = \lambda_{\mathrm{c}}\left(\frac{\partial T}{\partial x}\right)_{W}^{n+\theta} - \lambda_{\mathrm{c}}\left(\frac{\partial T}{\partial x}\right)_{\mathrm{E}}^{n+\theta} \tag{11}$$

For the virgin layer equation (10) becomes:

$$\rho_v c_v \frac{T^{n+1}\Delta x^{n+1} - T^n \Delta x^n}{\Delta t} + \rho_v c_v (T_W^{n-\theta} w_W^{n+1/2} - T_E^{n+\theta} w_E^{n+1/2}) = \lambda_v \left(\frac{\partial T}{\partial x}\right)_W^{n+\theta} - \lambda_v \left(\frac{\partial T}{\partial x}\right)_E^{n+\theta} \quad (12)$$

The temperature at the west boundary is computed as follows:

$$\begin{aligned} T_W^{n+1/2} &= (T_i^{n+1/2} + T_{i-1}^{n+1/2})/2 \\ &= \theta \cdot (T_i^{n+1} + T_{i-1}^{n+1})/2 + (1-\theta) \cdot (T_i^n + T_{i-1}^n)/2 \end{aligned} \quad (13)$$

and in a similar way for the east boundary:

$$\begin{aligned} T_E^{n+1/2} &= (T_i^{n+1/2} + T_{i+1}^{n+1/2})/2 \\ &= \theta \cdot (T_i^{n+1} + T_{i+1}^{n+1})/2 + (1-\theta) \cdot (T_i^n + T_{i+1}^n)/2 \end{aligned} \quad (14)$$

For the first pyrolysis time step, that is fully implicit, θ should be taken unity (backward Euler method), otherwise it is 1/2 (Cranck-Nicholson). Central space discretization is preferred above upwind as the mesh velocity is small and as there is no real strong convective flow.

Uniform grid in char layer

The grid of the char layer is kept equidistant because the temperature varies almost linearly in this zone. The velocity of the cell boundaries is determined by the velocity of the pyrolysis front. For a volume i in the char layer (numbering starts at 1 for the first volume):

$$\begin{cases} w_W^{n+1/2} = \dfrac{1}{N_c} \cdot \dfrac{\delta^{n+1} - \delta^n}{\Delta t} \cdot (i-1) \\ w_E^{n+1/2} = \dfrac{1}{N_c} \cdot \dfrac{\delta^{n+1} - \delta^n}{\Delta t} \cdot (i) \end{cases} \quad (15)$$

Uniform grid in virgin layer

For a uniform grid in the virgin layer the velocities of the mesh boundaries for a volume i (numbering starts at 1 for the first volume) are given by:

$$\begin{cases} w_{\mathrm{W}}^{n+1/2} = \dfrac{1}{N_{\mathrm{v}}} \cdot \dfrac{\delta^{n+1} - \delta^{n}}{\Delta t} \cdot (N_{\mathrm{v}} - i + 1) \\ w_{\mathrm{E}}^{n+1/2} = \dfrac{1}{N_{\mathrm{v}}} \cdot \dfrac{\delta^{n+1} - \delta^{n}}{\Delta t} \cdot (N_{\mathrm{v}} - i) \end{cases} \tag{16}$$

Non uniform grid in virgin layer

When stretching is used in the virgin layer, the size of a cell is equal to the length of the previous cell multiplied by a growth factor a. The factor is kept constant during the simulation. The size of cell i, Δx_i, can be written in function of the size of the first cell, Δx_1 (see Figure 3):

$$\Delta x_{\mathrm{i}} = a^{(i-1)} \cdot \Delta x_1 \tag{17}$$

The velocity of the mesh boundaries of the virgin volumes is again determined by the velocity of the pyrolysis front, and the location of the mesh boundaries. For volume i (numbering starts at 1 for the first volume) the velocity at the west boundary is given by:

$$w_{\mathrm{W}}^{n+1/2} = 2 \cdot \frac{\delta^{n+1} - \delta^{n}}{\Delta t} \cdot \frac{a^{i-1} - a^{N_{\mathrm{v}}}}{3 - a - 2a^{N_{\mathrm{v}}}} \tag{18}$$

and for the east boundary:

$$w_{\mathrm{E}}^{n+1/2} = 2 \cdot \frac{\delta^{n+1} - \delta^{n}}{\Delta t} \cdot \frac{a^{i} - a^{N_{\mathrm{v}}}}{3 - a - 2a^{N_{\mathrm{v}}}} \tag{19}$$

Solution of discretized equations

The discretized equations for one zone result in a tridiagonal matrix. This matrix is solved with the Thomas algorithm (Anderson *et al.*, 1984). To obtain the global solution an iterative method is used. In successive iterations the velocity of the pyrolysis front is corrected until the heat flux balance for the front is satisfied.

Even when there is no pyrolysis, an iterative method is required as the left boundary condition is nonlinear, caused by the radiation. A convergence criterion is based on the node temperatures (see *convergence criteria*).

Results moving grid model

The model will be implemented in a CFD code and act as a boundary condition. For this use, the most important results of the solid model are the surface temperature and the mass flux of the pyrolysis gasses. The material parameters that were used in the simulations are given in Table I.

The emissivity of the solid was assumed equal to 1. The thickness of the solid was in all cases 3 cm. Constant and variable external heat fluxes are applied.

Grid converged solution

The grid converged solution is obtained when the results of the simulation do not change anymore after grid refinement and time step size reduction.

When the grid and time step are refined, care should be taken that the numerical representation of the variables (temperatures) is accurate enough. When pyrolysis starts the char zone is very small, and when the time step size tends to zero the char zone will reduce to zero thickness as well. This is due to the singularity at the start of the pyrolysis phase. As a result, the difference between the temperatures of the nodes will decrease, as will the size of the char cells. When then the heat fluxes are calculated, problems of numerical accuracy can arise. The temperatures were stored with double precision. With the time steps and cell sizes examined here, no problems concerning accuracy came across.

Convergence criteria

The test for convergence uses all node temperatures. When the difference of the node temperature in successive iterations becomes smaller than a prescribed percentage of the actual node value, the time step is considered to be converged. Differences should certainly be smaller than 10^{-5} per cent. If larger, the time of extinguishment is predicted wrongly. The peak in the mass flux of pyrolysis gasses is still predicted well for a 10^{-2} per cent convergence criterion, but the time of extinguishment is strongly overpredicted due to the accumulation of the error in the released pyrolysis gasses during the simulation.

Dependent on the application of the results, severe or loose convergence criteria can be applied. If only the first minutes are of interest, the convergence criterion can be taken maximum 10^{-3} per cent to be on the safe side. If the time of extinguishment is important, it should be reduced to 10^{-8} per cent. For time steps of 0.01 s and 0.1 s, about ten iterations are necessary for each time step.

As in most applications the first minutes of pyrolysis are important, the peak in the mass flux of pyrolysis gasses will be used as criterion for grid optimization.

ρ_v [kg/m^3]	ρ_c [kg/m^3]	c_c [J/kg.K]	c_v [J/kg.K]	λ_v [W/m.K]	λ_c [W/m.K]	ΔH_{pyr} [J/kg]	T_{pyr} [°C]
650	350	1257	1257	0.1257	0.1257	7.54 10^5	300

Source: Karpov and Bulgakov (1994)

Table I.
Material properties

Number of volumes and size of the time step for the uniform grid in virgin layer
The number of volumes in the char and virgin layer and the time step length have been varied to find the optimal combination. When less volumes and larger time steps can be used, less calculation time is needed.

The number of volumes in the char and virgin layer is taken different. For the uniform grid, a grid converged solution can be obtained for only 4 volumes in the char layer and 64 in the virgin material. The temperature profile in the char layer is during pyrolysis almost linear so few cells are needed. On the other hand, the temperature profile in the shrinking virgin layer is better described by an error function (Carslaw and Jaeger, 1959), so more cells are required.

For the material properties used here, the time step should be smaller than or equal to 0.1 s.

Number of volumes and time step size for the non uniform grid in virgin layer
As the temperature is varying a lot near the pyrolysis front, the volumes should be small in that zone. Further away, the volumes can be larger. So, with a non-uniform grid less cells can be used for the virgin material. From Table II it can be concluded that 16 cells is the minimal number and a ratio from 10 to 40 can be used. If the number of cells is reduced further, the error in the peak of mass flux becomes larger than 1 per cent. The error in the mass flux is then not only significant at the peak, but also over the rest of the time interval.

Heating of pyrolysis gasses
The pyrolysis gasses that are produced at the pyrolysis front flow immediately out of the solid. When they flow through the char layer they can absorb energy of the solid. The influence of this effect is shown in Figures 4, 5, 6 and 7. The solid line shows the results when the volatiles do not absorb any energy in the char layer. This is done by setting the thermal heat capacity of the pyrolysis gasses c_g zero in equation (11). For the dashed line, the volatiles were always in thermal equilibrium with the solid they were flowing through. When the volatiles can absorb energy, more heat is lost by the solid. Subsequent, extinguishment is postponed and the peak in the mass flux of pyrolysis gasses is less high.

Table II.
Error for peak in mass flux of pyrolysis gasses [%] (n: number of cells; r: ratio = $\Delta x_{Nv}/\Delta x_1$; see Figure 3)

	R					
N	1	5	10	20	40	80
64	*0.2*	0.005	–	–	–	–
32	2.2	*0.2*	0.1	0.1	0.1	0.1
16	47.8	1.2	*0.5*	0.4	0.4	0.6
8	91.2	27.9	3.9	2.1	2.0	2.7
4	118.4	75.9	75.9	11.6	12.3	6.6

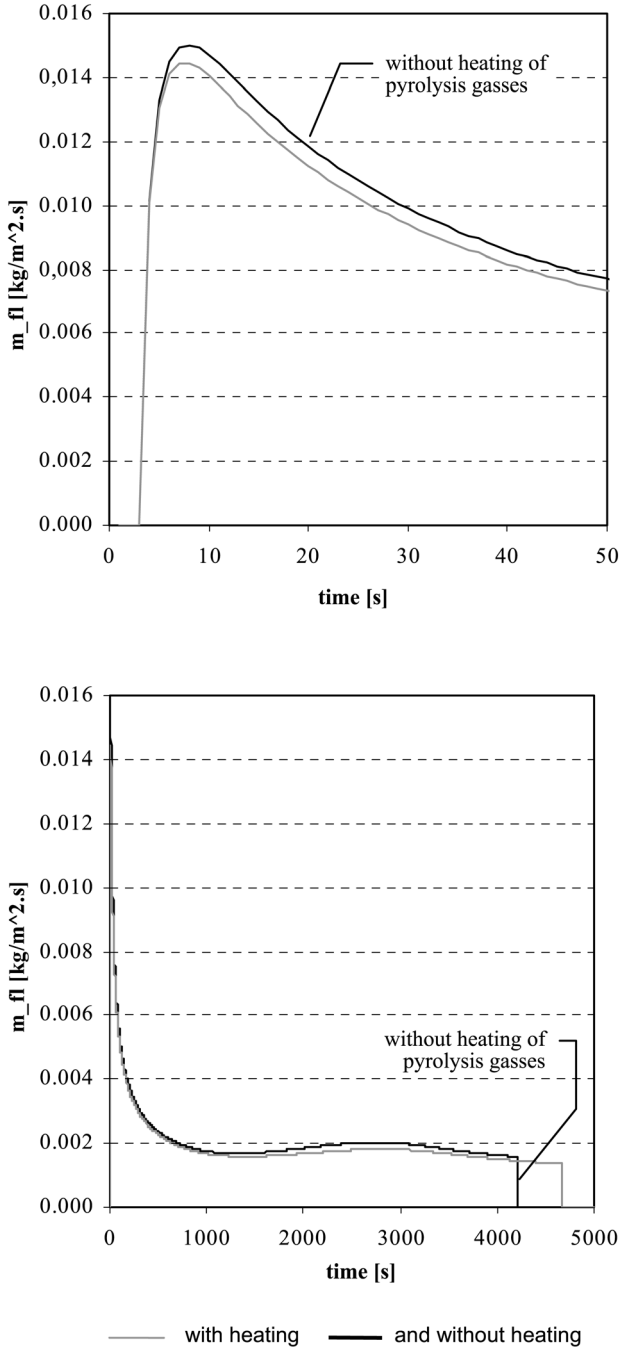

Figure 4.
Mass flux of pyrolysis gasses with (—)and without heating (—) Left: time 0 to 50 s; Right: time 0 to 5000 s

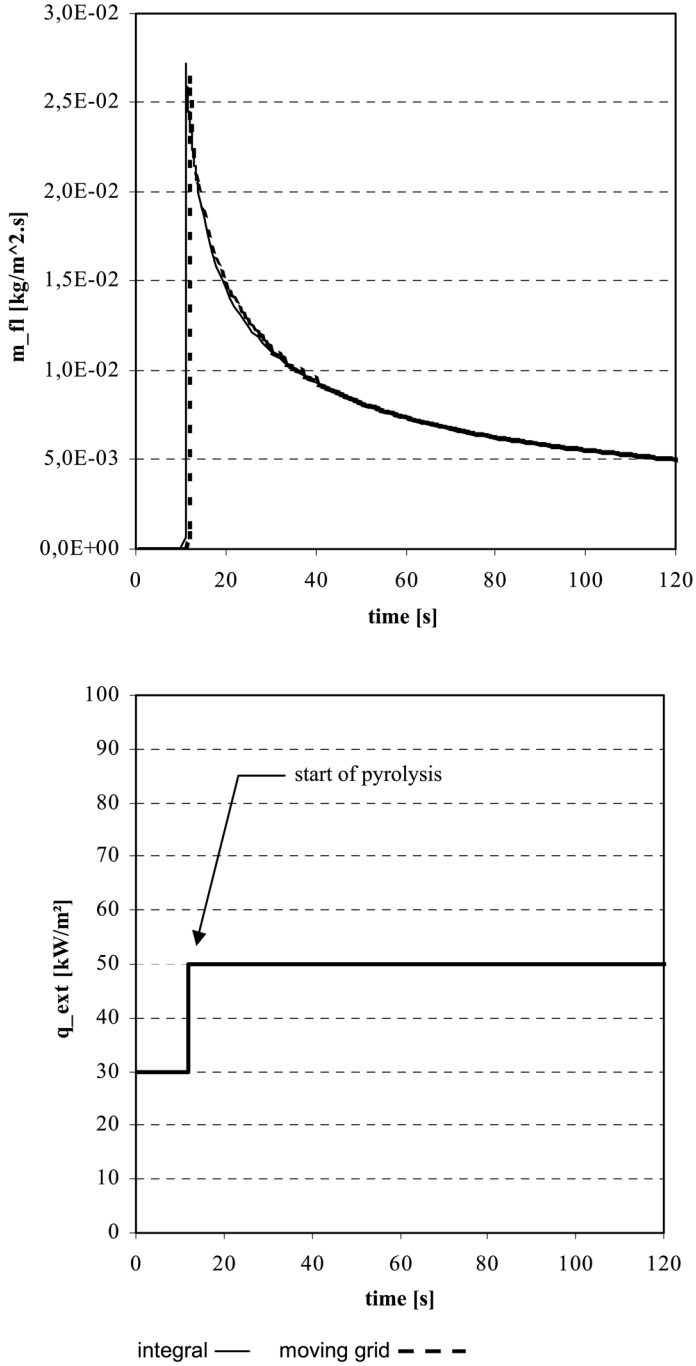

Figure 5.
Left: Mass flux of pyrolysis gasses (case 1); integral (—) moving grid (- -) Right: External heat flux

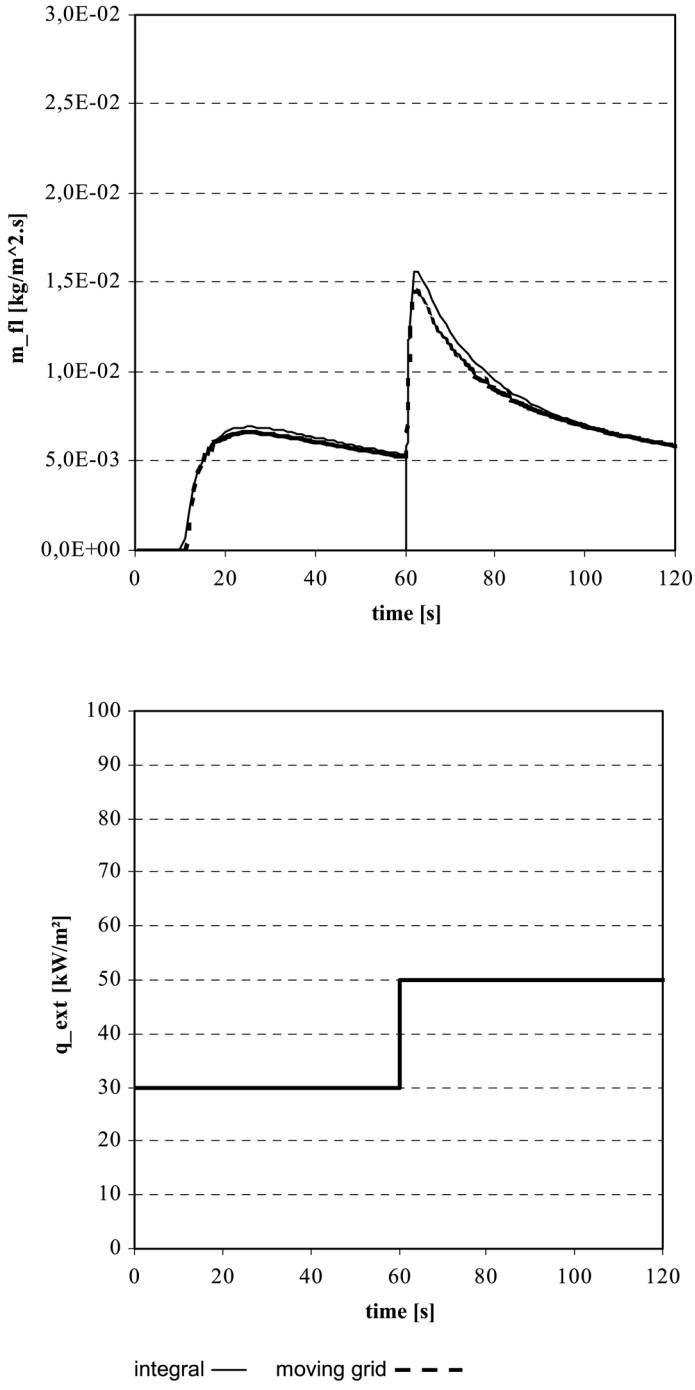

Figure 6.
Left: Mass flux of pyrolysis gasses (case 2); integral (—) moving grid (- -) Right: External heat flux

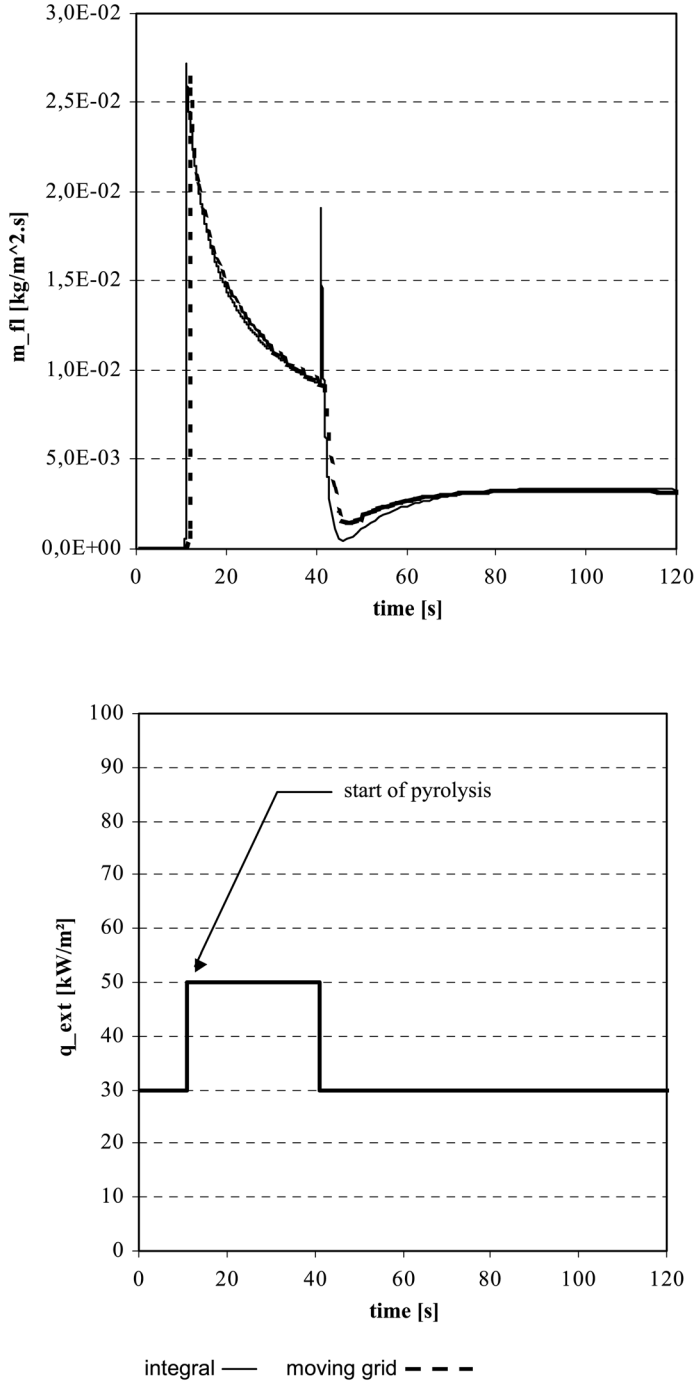

Figure 7.
Left: Mass flux of pyrolysis gasses (case 3); integral (—) moving grid (- -) Right: External heat flux

After about 1600s, the mass flux rises for both cases. This is due to the influence of the boundary condition at the back surface. Since that surface is isolated, the temperature in the virgin layer will continuously rise. As a result, less energy is required for heating up the virgin material to the pyrolysis temperature. On the other hand, when the pyrolysis front moves towards the back surface, the char layer thickens and has a larger thermal resistance. Less energy will be supplied to the pyrolysis front. The result of these two phenomena is known as the back effect.

Comparison with the integral model of Moghtaderi *et al.* (1997)

Instead of solving the integral equations with a finite volume technique, it is also possible to prescribe the temperature profile in the solid. A linear or quadratic profile for the char layer, and an exponential or quadratic profile for the virgin layer can be used (Moghtaderi *et al.*, 1997), (Delichatsios *et al.*, 1991). With the boundary conditions, and the conservation equations of energy for the virgin and char zone, the unknown coefficients of the temperature profiles can be determined. The problem can be reduced to a system of three differential equations in three unknowns. In literature, this method is known as the integral model. To avoid confusion with the integral Equations (3) and (5), quotation marks are used for the approximate "integral model". Details about the "integral model" can be found in (Moghtaderi *et al.*, 1997). The moving grid model will be compared with an "integral model" where both in the char and in the virgin layer a quadratic temperature profile is used. Four cases, with different external heat fluxes, are examined. All cases tend to represent a realistic event, typical for enclosure fires.

The "integral model" has already been compared with experimental data (Moghtaderi *et al.*, 1997) (Spearpoint and Quintiere, 2000). However, this comparison is hampered by the modelling of the experiment itself because the net incident heat flux must always be modelled somehow. Therefore, the difference between the experiments and the simulation can be due to the prescribed temperature profile in the "integral model" or due to the representation of the experiment (definition of material properties or the modelling of the boundary condition of the solid). When the "integral model" is compared with the moving grid method, a mathematical validation can be done because both use the exact same physical model and the same boundary conditions.

Case 1: Single step function. When the pyrolysis starts and combustible volatiles are released (in the moving grid model after 12 s) the external heat flux is raised from 30 to 50 kW/m^2. The constant heat flux of 30 kW/m^2 represents the radiation from remote flames or from test radiation panels. The increase in the incident heat flux represents the ignition of the combustible volatiles in the

gas phase and can be seen as a persistent flame. The induction time to obtain an ignitable mixture in the gas phase, is neglected. The rise in the external heat flux is triggered by the first release of pyrolysis gasses, which happens when the surface temperature reaches the critical pyrolysis temperature.

Both models give similar results. There are minor differences in the peak of the mass flux of pyrolysis gasses and the time at which this peak occurs.

Case 2: Sudden increase. For enclosed fires flashover can occur. When a flashover takes place, all the exposed combustible items in the enclosure get involved. This phenomenon is here modelled as a sudden rise in the external heat flux some time after the start of pyrolysis. In this case, the rise in the external heat flux happens on a fixed time (60 s after start). In reality, the time of flashover is dependent on the enclosure conditions.

The peak in the release of pyrolysis gasses is much lower than in case 1, because of the insulating effect of the char layer. When the external heat flux rises, the char layer is already much thicker than in case 1 so heat transfer to the pyrolysis front is delayed.

The "integral model" shows some peculiar behaviour: immediately after the rise of the external heat flux the mass flux of pyrolysis gasses drops sharply. In some cases even negative mass fluxes where noted. The reason therefore is the unrealistic, direct influence of the net incident heat flux on the whole temperature profile. This sudden decrease in the mass flux of pyrolysis gasses is not present in case 1 as the change in the external heat flux happens just at the start of pyrolysis.

Case 3: Crisp variation of external heat flux. In this case a sudden rise and fall of the external heat flux is examined. The rise in the external heat flux starts at the beginning of pyrolysis, while the fall is at a fixed time. The fall in the external heat flux can represent the extinghuisment of the flames in the gas phase due to, e.g. lack of oxygen, or the activation of a sprinkler installation.

Here the "integral model" shows again a bad prediction just after the fall of the external heat flux. There is a sudden rise in the mass flux of pyrolysis gasses, but less than a second later, the mass flux is back normal.

Case 4: Smooth variation of external heat flux. It is clear that the "integral model" has problems with sudden changes in the external heat flux. Therefore, in this case, the external heat flux is varied smoothly (sinusoidal for the variation between 30 and 50 kW/m^2).

As can be seen in Figure 8 when a smooth variation in the external heat flux is applied, the "integral model" shows good agreement with the moving grid model.

When calculation times are compared, the "integral model" is in general about 5 times faster than the moving grid model. When a coarse mesh and larger time steps are taken, the calculation time of the moving grid will of course decrease, but the results will be less accurate.

Deficiencies of "integral model"

The "integral model" performs very well when the boundary conditions are constant or changing slowly. Sudden changes in the net incident heat flux, though, are transmitted immediately and unrealistically high through the entire solid.

As the temperature is prescribed (e.g. quadratic), the "integral model" can only be valid for those types of heating that will result in that prescribed temperature profile. In flame spread simulations the incident heat flux can suddenly rise due to for example ignition of the pyrolysis gasses in the gas phase, but it can also suddenly fall due to for example lack of oxygen in the gas phase. This kind of heating can result in temperature profiles that are different from the quadratic ones.

As the moving grid model permits grid refinement it will converge to the correct solution of the model equations. The "integral model" on the other side has not the capability to refine and consequently will always give an approximate solution of these model equations.

A last advantage of the moving grid model is the possibility to expand the method to two or three dimensions. In the "integral model" only one dimensional heat transfer is allowed and thus a more dimensional pyrolysis problem can only be solved as a series of independent one dimensional problems.

Conclusion

The moving grid technique has been used for the solution of the one dimensional pyrolysis of charring solids. The solid is separated into two zones: a char layer and unaffected virgin material. The movement of the grid is determined by the advancing, infinitely thin pyrolysis front and the steady boundaries of the solid. Of the two grids examined, the non-uniform is preferred above the uniform. About 4 times less cells are needed for the non uniform grid which give calculation times that are about 3 times faster. The growth factor in the non-uniform grid can be taken very large. Values up to 1.2 are still acceptable. In the char layer few cells are required because of the almost linear temperature profile.

"Integral models" are not always capable of giving correct or realistic results. Sudden changes in the boundary conditions can give temporarily

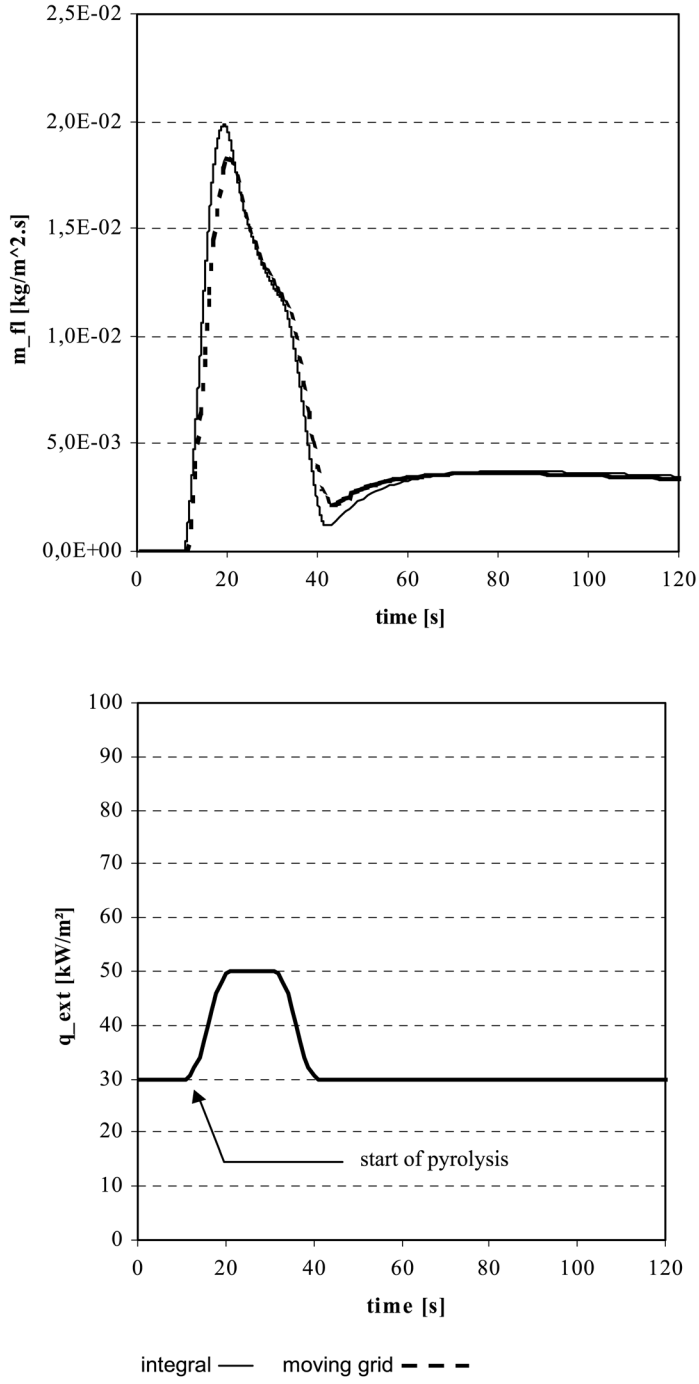

Figure 8.
Left: Mass flux of pyrolysis gasses (case 3); integral (—) moving grid (- -) Right: External heat flux

unrealistic results, though the "integral model" recovers quickly. When large time steps are taken, these effects can be camouflaged.

Errors in the mass flux of pyrolysis gasses are largest for sudden changes in the external heat flux and at peak values of the mass flux. Maximum peak errors, dependent on the way of heating, are about 8 per cent.

If calculation time is important and the boundary conditions change smoothly the "integral model" should be preferred. When the boundary conditions can vary abruptly or when they can lead to non-quadratic temperature profiles in the solid, the moving grid method should be used.

References

Anderson D.A., Tannchill J.C. and Pletchen R.H. (1984), *Computational Fluid Mechanics and Heat Transfer*, ISBN 0 07 050328 1, Hemisphere publishing corporation, p. 599.

Carslaw, H.S. and Jaeger, J.C. (1959), *Conduction of heat in solids*, Oxford University Press, London 510 pp.

Croft, D.R. and Lilley, D.G. (1977), *Heat transfer calculations using finite difference equations*, ISBN 0-85334-720-4, Applied Science Publishers LTD, Ripple Road, Barking Essex, England 283 pp.

Di Blasi, C. (1994), "Processes of flames spreading over the surface of charring solid fuels: effects of fuel thickness", *Combustion and Flame*, Vol. 97, pp. 225-39.

Delichatsios, M.M., Mathews, M.K. and Delichatsios, M.A. (1991), "An upward fire spread and growth simulation", in, *Fire Safety Science – Proceedings of the Third International Symposium*, Cox, G., Langford, B., (Eds) p. 1045 Elsevier Applied Science, N.Y. pp. 207-16.

Karpov, A.I. and Bulgakov, V.K. (1994), "Prediction of the steady rate of flame spread over combustible materials", in, *Fire Safety Science – Proceedings of the Fourth International Symposium*, Kashiwagi, T., (Eds) pp. 373-84.

Moghtaderi, B., Novozhilov, V., Fletcher, D. and Kent, J.H. (1997), "An integral model for the transient pyrolysis of solid materials", *Fire and Materials*, Vol. 21, pp. 7-16.

Staggs, J.E.J. (2000), "A simple model of polymer pyrolysis including transport of volatiles", *Fire Safety Journal*, Vol. 34, pp. 69-80.

Spearpoint, M.J. and Quintiere, J.G. (2000), "Predicting the burning of wood using an integral model", *Combustion and Flame*, Vol. 123, pp. 308-24.

Tewarson, A. (1995), *SFPE handbook of Fire Engineering*, 2nd edition, Society of Fire Protection Engineers, Boston, MA pp. 35-3-3-124.

Yan, Z. and Holmstedt, G. (1997), "CFD simulation of upward flame spread over fuel surface", *Fire Safety Science- Proceedings of the Fifth International Symposium*, pp. 345-56.